

Density Ratio-based Causal Discovery from Bivariate Continuous-Discrete Data

Takashi Nicholas Maeda^{1,3,4}, Shohei Shimizu^{2,3,4}, Hidetoshi Matsui³

¹Gakushuin University, Tokyo, Japan ²The University of Osaka, Osaka, Japan

³Shiga University, Shiga, Japan ⁴RIKEN, Tokyo, Japan

Abstract

This paper proposes a causal discovery method for mixed bivariate data consisting of one continuous and one discrete variable. Existing constraint-based approaches are ineffective in the bivariate setting, as they rely on conditional independence tests that are not suited to bivariate data. Score-based methods either impose strong distributional assumptions or face challenges in fairly comparing causal directions between variables of different types, due to differences in their information content. We introduce a novel approach that determines causal direction by analyzing the monotonicity of the conditional density ratio of the continuous variable, conditioned on different values of the discrete variable. Our theoretical analysis shows that the conditional density ratio exhibits monotonicity when the continuous variable causes the discrete variable, but not in the reverse direction. This property provides a principled basis for comparing causal directions between variables of different types, free from strong distributional assumptions and bias arising from differences in their information content. We demonstrate its effectiveness through experiments on both synthetic and real-world datasets, showing superior accuracy compared to existing methods.

1 Introduction

Determining the causal relationship between continuous and discrete variables using observational data alone is both crucial and challenging in many real-world scenarios. Consider, for instance, the relationship between a biological marker in the body (a continuous variable) and the development of a specific medical condition (a discrete variable). It can be difficult to ascertain whether changes in the biological marker lead to the onset of the medical condition or if early-stage disease processes alter the biological marker’s levels. Although randomized controlled trials (RCTs) are reliable, they are often infeasible due to ethical, logistical, or financial constraints.

The method of estimating causal relationships between variables from observational data without conducting experiments is called *causal discovery* [20, 27, 6]. The process involves three key steps: first, establishing specific assumptions about the data-generating process (termed a *causal model*); second, proving that causal relationships are identifiable under these assumptions; and finally, developing methods to estimate causal relationships based on this theoretical identifiability.

Causal discovery methods can be broadly categorized into constraint-based [26, 28] and score-based [3, 25] approaches. Constraint-based methods identify causal relationships through conditional independence tests between variables, while score-based methods evaluate different causal structures using model scoring functions to find the optimal model. Both approaches have been applied to mixed data containing discrete and continuous variables [30, 4, 5, 32, 35,

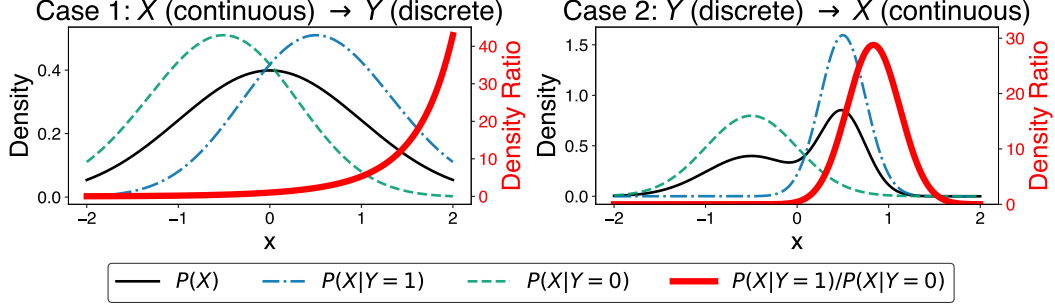


Figure 1: Monotonicity property of the density ratio. The figure illustrates our key finding: when a continuous variable (X) causes a discrete variable (Y) (Case 1, left), the conditional density ratio $\frac{P(X|Y=1)}{P(X|Y=0)}$ (red line) exhibits monotonic behavior. In contrast, when the causal direction is reversed and a discrete variable (Y) causes a continuous variable (X) (Case 2, right), this monotonicity property does not hold.

15, 17, 16]. However, for bivariate mixed data, constraint-based methods fail because they rely on conditional independence tests that require more than two variables. Score-based methods also struggle with restrictive distributional assumptions and difficulties in fairly comparing models with different causal directions due to inherent differences in information content between variable types.

This paper proposes a method for estimating causal relationships from bivariate data consisting of one continuous and one discrete variable. Our framework relaxes the distributional assumptions on exogenous variables required by current approaches. We establish a crucial property relating the causal direction and the behavior of conditional density ratios. Specifically, when a continuous variable X causes a discrete variable Y , the ratio of conditional probability densities $\frac{P(X|Y=c_t)}{P(X|Y=c_s)}$ exhibits monotonic behavior. Conversely, when a discrete variable Y causes a continuous variable X , this density ratio does not exhibit monotonicity. This pattern is illustrated in Figure 1. While this figure was generated using specific settings (detailed in Appendix B), our theoretical results hold more generally as demonstrated throughout this paper. By focusing solely on the monotonicity of the density ratio, our method naturally addresses the fundamental challenge of comparing models in different causal directions (continuous \rightarrow discrete versus discrete \rightarrow continuous). This eliminates the need for ad hoc normalization techniques used in existing methods that lack theoretical justification. Consequently, we can identify causality between two variables under minimal assumptions about the underlying probability distributions.

The main contributions of this paper are as follows: (1) We establish a theoretical property that enables the identification of the causal relationship between a continuous variable and a discrete variable by examining the monotonicity of the conditional density ratio; (2) Based on this property, we develop a novel approach, called *Density Ratio-based Causal Discovery* (DRCD), which identifies causal relationships from bivariate mixed data while avoiding restrictive distributional assumptions and ad hoc normalization when comparing different causal directions; (3) We demonstrate, through experiments on both synthetic and real-world datasets, that our method consistently outperforms existing methods.

For our theoretical results (Lemmas 1, 2, and 3), we provide brief proof sketches in the main text to highlight the key intuition, while detailed proofs are presented in Appendix A. The complete proofs of Lemma 4 and Theorem 1 are provided directly in the main text due to their brevity. Code is available at <https://github.com/causal111/DRCD>.

2 Related Studies

We organize causal discovery methods into constraint-based, model-driven, and flexible score-based approaches, and consider the limitations of each in handling mixed data.

Constraint-based approaches. Constraint-based methods determine causal directions by testing whether pairs of variables satisfy conditions that should hold under causal relationships. Existing constraint-based approaches including PC [26] and FCI [28] make the Faithfulness assumption [20] and estimate causal relationships based on conditional independence. Methods that can be applied to mixed data have been proposed within this approach [30, 4, 5]. However, in the case of data with only two variables having a causal relationship, it is not possible to identify its direction from conditional independence. Therefore, while constraint-based methods have proven effective for multivariate causal discovery, their application to bivariate mixed data remains an open challenge.

Model-driven approaches. Model-driven approaches estimate causal structure by assuming specific functional relationships or noise structures and searching for models that optimize statistical criteria. LiNGAM [24] assumes a linear model with non-Gaussian noise and identifies a causal ordering using independent component analysis. Additive noise models (ANM) [7, 22] generalize this idea to nonlinear functions under the assumption that the noise is statistically independent of the input. Building on these foundations, several methods extend this line of work to mixed data by formulating score-based frameworks under specific distributional assumptions. For example, MIC [32] and LiM [35] define likelihood-based scores under explicit assumptions about the distributions of noise terms. When continuous variable X causes binary variable Y , they model $Y = 1$ if $a_X X + N_Y > 0$ and $Y = 0$ otherwise, and $X = a_Y Y + N_X$ when Y causes X . The score functions are then computed assuming that N_Y follows a logistic distribution and N_X follows a Laplace distribution.

Flexible score-based methods with minimal assumptions. Several recent score-based approaches have been developed to address causal discovery while minimizing assumptions about the functional form of causal mechanisms or the distribution of noise terms. For continuous variables, methods such as SLOPE [15] and SLOPPY [17] determine causal relationships using the minimum description length (MDL) principle. For mixed data, CRACK [16] extends this MDL approach using regression and classification trees to encode dependencies. Meanwhile, HCM [13] and GSF [8] take different methodological directions; the former combining constraint-based and score-based reasoning with cross-validation, and the latter defining score functions in reproducing kernel Hilbert space for nonparametric modeling. These methods represent significant advances toward more flexible causal discovery from mixed data, without requiring strong assumptions about the functional form or distribution of the data-generating process. Nonetheless, a fundamental difficulty remains in fairly comparing causal directions between continuous and discrete variables, due to inherent differences in information content and scale between variable types.

Challenges in existing methods. Existing score-based methods for causal discovery from mixed data face several significant challenges. First, some methods such as MIC [32] and LiM [35] define scoring functions based on specific probability distribution assumptions for the causal model variables. This approach creates vulnerability to incorrect estimations when applied to real-world data that do not satisfy these underlying assumptions. Second, the inherent differences in information content and scale between continuous and discrete variables make it difficult to fairly evaluate competing causal models, particularly when comparing models where continuous variables cause discrete variables versus models where discrete variables cause continuous variables. While methods like MIC [32] and CRACK [16] incorporate scale adjustment techniques, these approaches lack sufficient theoretical justification. Third, several methods including MIC [32], LiM [35], HCM [13], and GSF [8] use complexity penalties to determine the absence of causal relationships between variable pairs. However, establishing valid parameter settings for these penalties remains challenging.

Our focus on bivariate cases. Existing causal discovery methods for mixed data are primarily designed for multivariate scenarios with three or more variables. However, in other settings of causal discovery beyond mixed data, significant theoretical advances have been achieved by deliberately focusing on bivariate cases [1, 18, 10, 29, 2, 21, 33, 23]. This focused approach has enabled the development of clear identifiability theories and effective methods, even when extension to multivariate contexts was not immediately obvious. Our work follows this successful strategy for mixed data scenarios, specifically addressing the case of one continuous and one discrete variable to overcome the fundamental limitations faced by existing methods for mixed data.

3 Model

For a continuous variable X and a discrete variable Y , we consider three possible causal models: (1) X causes Y , (2) Y causes X , or (3) no causal relationship exists.

3.1 The model where X is the cause of Y

We consider a causal model in which the random variables X and Y satisfy

$$X = N_X, \quad Y = f(X, \mathbf{N}_Y), \quad (1)$$

where N_X is a continuous random variable, $\mathbf{N}_Y = \{N_{Y,i}\}_i$ is a collection of continuous random variables, and N_X is independent of every $N_{Y,i} \in \mathbf{N}_Y$. In this model, the function f represents the mapping from X to Y , incorporating noise variables \mathbf{N}_Y . The function f is structured as follows:

$$f_i(X, N_{Y,i}) = \begin{cases} f_{2i}(X, N_{Y,2i}) & \text{if } a_i X + N_{Y,i} \geq b_i, \\ f_{2i+1}(X, N_{Y,2i+1}) & \text{otherwise,} \end{cases} \quad (2)$$

where a_i and b_i are fixed constants (with $a_i \neq 0$ to ensure X influences the outcome). At terminal points in this mapping, the function assigns a discrete value:

$$f_i(X, N_{Y,i}) = c_i. \quad (3)$$

This formulation represents a natural extension of the binary variable models used in MIC [32] and LiM [35] to accommodate discrete variables with multiple values. The natural interpretation here is that any pair of discrete values can be distinguished by at least one decision boundary of the form $a_i X + N_{Y,i} \geq b_i$ within the tree-structured model.

3.2 The model where Y is the cause of X

The causal model in this case is given by

$$X = \sum_{k=1}^n \delta(c_k, Y) N_{X,k}, \quad Y = N_Y, \quad (4)$$

where N_Y is a discrete-valued random variable with $P(N_Y = c_k) = p_k$ such that $\sum_k p_k = 1$, each $N_{X,k}$ is a random variable, and $\delta(c_i, Y)$ is the indicator function (equals 1 if $Y = c_i$, 0 otherwise). We impose the following assumption on the collection $\{N_{X,k}\}$: For each k , let g_k be defined by $P(N_{X,k} = x) = \exp(g_k(x))$. Then, for any $i \neq j$, we assume that

$$\lim_{x \rightarrow \infty} \frac{g_i(x)}{g_j(x)} \neq 1 \quad \text{and} \quad \lim_{x \rightarrow -\infty} \frac{g_i(x)}{g_j(x)} \neq 1. \quad (5)$$

In addition, we assume that each $N_{X,k}$ satisfies the *Tail Symmetry of a Random Variable* (TSRV) condition, defined as follows.

Definition 1 (Tail Symmetry of a Random Variable (TSRV)). *Let the probability density function of a random variable X be given by $P_X(x) = \exp(f(x))$. We say that X satisfies the TSRV property if*

$$\lim_{x \rightarrow \pm\infty} f(x) = -\infty \quad \text{and} \quad \lim_{x \rightarrow \infty} \frac{f(x)}{f(-x)} = 1. \quad (6)$$

The TSRV condition only places constraints on the asymptotic behavior of distributions as x approaches $\pm\infty$, with no restrictions on their shape or characteristics in central regions. Various probability distributions satisfy this condition, including the Laplace distribution, the Gaussian distribution, the t -distribution, and the generalized Gaussian distribution. The following lemma shows that the TSRV property is preserved under mixtures.

Lemma 1 (Closure of TSRV under mixtures). *Let X_1, X_2, \dots, X_n be random variables that all satisfy the TSRV condition. If the probability density function of a random variable X is given by*

$$P_X(x) = \sum_{i=1}^n \omega_i P_{X_i}(x), \quad (7)$$

with $\omega_i > 0$ and $\sum_{i=1}^n \omega_i = 1$, then X also satisfies the TSRV condition.

Proof sketch. Express the probability density functions in exponential form: $P_X(x) = \exp(f(x))$, $P_{X_i}(x) = \exp(g_i(x))$ for $i = 1, 2, \dots, n$. From the definition of the mixture distribution: $\exp(f(x)) = \sum_{i=1}^n \omega_i \exp(g_i(x))$. Taking logarithms: $f(x) = \log(\sum_{i=1}^n \omega_i \exp(g_i(x)))$. Define $M(x) = \max\{g_1(x), g_2(x), \dots, g_n(x)\}$. Since all X_i satisfy the TSRV condition, we can prove that: $\lim_{x \rightarrow \infty} \frac{M(x)}{M(-x)} = 1$. By manipulating the expression for $f(x)$, we can show that: $f(x) = M(x) + O(1)$ and $f(-x) = M(-x) + O(1)$. Therefore: $\lim_{x \rightarrow \infty} \frac{f(x)}{f(-x)} = \lim_{x \rightarrow \infty} \frac{M(x) + O(1)}{M(-x) + O(1)} = \lim_{x \rightarrow \infty} \frac{M(x)}{M(-x)} = 1$. Hence, the mixture distribution X also satisfies the TSRV condition.

3.3 The model with no causal relationship

In the case where there is no causal relationship between X and Y , the model is given by

$$X = N_X, \quad Y = N_Y, \quad (8)$$

where N_X is a continuous random variable and N_Y is a discrete-valued random variable. We assume that N_X and N_Y are independent.

4 Identifiability

This section establishes that the causal relationship between a continuous variable X and a discrete variable Y is identifiable under the modeling assumptions in Section 3. The key insight lies in the behavior of the density ratio

$$G_{c_s, c_t}(x) = \frac{p_{X|Y}(x | c_t)}{p_{X|Y}(x | c_s)}, \quad (9)$$

defined for any two distinct values c_s and c_t of Y . We show that this function exhibits different patterns (monotonicity, non-monotonicity, or constancy) depending on whether $X \rightarrow Y$, $Y \rightarrow X$, or no causal relationship exists. These properties are formalized in the following lemmas and lead to our main identifiability result.

Definition 2 (Monotonicity). Throughout this paper, we use the term **monotonic** to refer exclusively to functions that are non-decreasing or non-increasing but not constant. Specifically, a function f is called **monotonic** if either (1) for all $x_0 < x_1$, $f(x_0) \leq f(x_1)$ and $f(-\infty) < f(\infty)$, or (2) for all $x_0 < x_1$, $f(x_0) \geq f(x_1)$ and $f(-\infty) > f(\infty)$.

Definition 3 (Non-monotonicity). A function f is called **non-monotonic** if it is neither monotonic nor constant. Specifically, a function f is non-monotonic if and only if there exist points $x_0 < x_1 < x_2$ such that $(f(x_0) - f(x_1))(f(x_1) - f(x_2)) < 0$.

Lemma 2 (Monotonicity of the density ratio under $X \rightarrow Y$). Assume that (X, Y) are generated according to the model described in Section 3.1 with the causal direction $X \rightarrow Y$. Then, for any distinct outcomes c_s and c_t of Y , the function $G_{c_s, c_t}(x)$ is **monotonic** in x . Additionally, $G_{c_s, c_t}(x)$ satisfies either $\lim_{x \rightarrow -\infty} G_{c_s, c_t}(x) = \infty$ and $\lim_{x \rightarrow \infty} G_{c_s, c_t}(x) = 0$, or $\lim_{x \rightarrow -\infty} G_{c_s, c_t}(x) = 0$ and $\lim_{x \rightarrow \infty} G_{c_s, c_t}(x) = \infty$.

Proof sketch. In our causal model where $X \rightarrow Y$, the output Y is generated by a binary decision tree. For any distinct outcomes c_s and c_t , there exists a decision node i that separates them through the condition $a_i x + N_{Y,i} \geq b_i$. Using Bayes' rule and the independence of $N_{Y,i}$ from X , we derive $p_{X|Y=c_s}(x) = \frac{H(b_i - a_i x)}{p_Y(c_s)} p_X(x) (p_Y(c_s) + p_Y(c_t))$ and $p_{X|Y=c_t}(x) = \frac{1 - H(b_i - a_i x)}{p_Y(c_t)} p_X(x) (p_Y(c_s) + p_Y(c_t))$, where H is the conditional CDF of $N_{Y,i}$ given $Y \in \{c_s, c_t\}$. The density ratio becomes $G_{c_s, c_t}(x) = A \cdot \frac{1 - H(b_i - a_i x)}{H(b_i - a_i x)}$ where $A = \frac{P(Y=c_s)}{P(Y=c_t)}$. Since H is monotonic (being a CDF) and $b_i - a_i x$ is affine in x , $G_{c_s, c_t}(x)$ is monotonic in x . Additionally, because H ranges from 0 to 1 as x varies, $G_{c_s, c_t}(x)$ satisfies either $\lim_{x \rightarrow -\infty} G_{c_s, c_t}(x) = \infty$ and $\lim_{x \rightarrow \infty} G_{c_s, c_t}(x) = 0$, or $\lim_{x \rightarrow -\infty} G_{c_s, c_t}(x) = 0$ and $\lim_{x \rightarrow \infty} G_{c_s, c_t}(x) = \infty$.

Lemma 3 (Non-monotonicity of the density ratio under $Y \rightarrow X$). Suppose that (X, Y) are generated according to the model described in Section 3.2 with the causal direction $Y \rightarrow X$.

Then, for any distinct c_s and c_t of Y , the function $G_{c_s, c_t}(x)$ is **non-monotonic** with respect to x . Additionally, $G_{c_s, c_t}(x)$ satisfies either $\lim_{x \rightarrow \pm\infty} G_{c_s, c_t}(x) = 0$ or $\lim_{x \rightarrow \pm\infty} G_{c_s, c_t}(x) = \infty$.

Proof sketch. In our model where $Y \rightarrow X$, we can express the density ratio as $G_{c_s, c_t}(x) = \frac{P(X=x|Y=c_t)}{P(X=x|Y=c_s)} = \frac{P_{N_{X,t}}(N_{X,t}=x)}{P_{N_{X,s}}(N_{X,s}=x)} = \exp(g_t(x) - g_s(x))$, where g_t and g_s are log-density functions. As stated in Section 3.2, we have $\lim_{x \rightarrow \infty} \frac{g_t(x)}{g_t(-x)} = \lim_{x \rightarrow \infty} \frac{g_s(x)}{g_s(-x)} = 1$, implying symmetric asymptotic behavior, and $\lim_{x \rightarrow \infty} \frac{g_t(x)}{g_s(x)} = L \neq 1$. Further, g_t and g_s both approach $-\infty$ as $|x| \rightarrow \infty$. We analyze $\exp(g_t(x) - g_s(x))$ for large $|x|$ by examining $\exp(g_s(x)(\frac{g_t(x)}{g_s(x)} - 1))$. When $L > 1$, we have $\lim_{x \rightarrow \pm\infty} G_{c_s, c_t}(x) = 0$. When $L < 1$, we have $\lim_{x \rightarrow \pm\infty} G_{c_s, c_t}(x) = \infty$. The ratio cannot be monotonic because it is not constantly 0 or ∞ over the entire real line.

Lemma 4 (Constant density ratio under no causal relationship). Suppose that (X, Y) are generated according to the model described in Section 3.3 with no causal relationship between X and Y . Then, for any two distinct c_s and c_t of Y , the function $G_{c_s, c_t}(x)$ is **constant** and equals 1 for all x .

Proof. Since X and Y have no causal relationship, they are statistically independent. By definition, independence means $p_{X|Y}(x|y) = p_X(x)$ for all x and y . Therefore, for any distinct c_s and c_t of Y : $G_{c_s, c_t}(x) = \frac{p_{X|Y}(x|c_t)}{p_{X|Y}(x|c_s)} = \frac{p_X(x)}{p_X(x)} = 1$. Thus, $G_{c_s, c_t}(x)$ equals 1 for all x . \square

Theorem 1 (Identifiability of the causal relationship). Assume that the joint distribution of (X, Y) is generated according to exactly one of the three causal models defined in Section 3: (1) $X \rightarrow Y$, (2) $Y \rightarrow X$, or (3) no causal relationship. Then, the causal relationship between X and Y is identifiable.

Proof. By Lemma 2, the density ratio function $G_{c_s, c_t}(x)$ is monotonic in x when $X \rightarrow Y$. By Lemma 3, it is non-monotonic when $Y \rightarrow X$. By Lemma 4, it is constant and equal to 1 when X and Y are independent. These three properties are mutually exclusive and exhaustive under the model class in Section 3, so the causal relationship is identifiable. \square

5 Method

We propose *Density Ratio-based Causal Discovery* (DRCD), a method for determining which of the three causal models best characterizes the relationship between a continuous variable X and a discrete variable Y : (1) X causes Y , (2) Y causes X , or (3) no causal relationship exists between X and Y . DRCD consists of three main steps: (1) testing for causal existence, (2) density ratio estimation, and (3) monotonicity evaluation for causal direction determination. The DRCD procedure is formalized in Algorithm 1. Below, we provide a detailed explanation of each step to clarify the theoretical foundations and implementation details.

Step 1: Testing for causal existence. To assess the existence of a causal relationship between X and Y , we examine whether the conditional distributions $p_{X|Y}(x|y)$ differ across values of y . When no causal relationship exists, X and Y are statistically independent, so these distributions should be identical. We use the two-sample Kolmogorov–Smirnov test to assess whether the distributions $p_{X|Y}(x|c_s)$ and $p_{X|Y}(x|c_t)$ differ significantly, where c_s and c_t are two distinct values of Y . We select the two most frequent values of Y as c_s and c_t . Although any distinct pair can be used in principle, we use such c_s and c_t , as this choice generally improves statistical reliability. If no significant difference is detected, we conclude that there is no causal relationship; otherwise, we proceed to determine the causal direction.

Step 2: Density ratio estimation and determining the valid domain for evaluation. Based on Lemmas 2 and 3, the monotonicity of the density ratio between conditional distributions determines the causal direction. We estimate the density ratio $G_{c_s, c_t}(x) = \frac{p_{X|Y}(x|c_t)}{p_{X|Y}(x|c_s)}$ using RuLSIF [34]. To ensure reliable estimation, we define a valid domain $[x_{\min}, x_{\max}]$ for evaluation, where $x_{\min} = \max\{\min\{X | Y = c_s\}, \min\{X | Y = c_t\}\}$ and $x_{\max} = \min\{\max\{X | Y = c_s\}, \max\{X | Y = c_t\}\}$. This restriction ensures that the evaluation region lies within the overlapping support of the two conditional distributions.

Step 3: Evaluating monotonicity to determine causal direction. We determine the causal direction by evaluating the monotonicity of the estimated density ratio $G_{c_s, c_t}(x)$. Within the evaluation region $[x_{\min}, x_{\max}]$, we construct an evenly spaced sequence $\mathcal{X} = (x_k)_{k=1}^{n_{\text{points}}}$ and compute the sequence of differences in the estimated density ratios, $\mathcal{D} = (G_{c_s, c_t}(x_k) - G_{c_s, c_t}(x_{k-1}))_{k=2}^{n_{\text{points}}}$. We apply a one-sample t -test to determine whether the mean of these differences significantly differs from zero. If the test indicates a statistically significant difference, we interpret this as evidence that the estimated density ratios $G_{c_s, c_t}(x)$ exhibit a monotonic pattern, and infer $X \rightarrow Y$. Otherwise, we infer $Y \rightarrow X$. Although the Mann–Kendall trend test [14, 12] is commonly used to detect monotonicity, it relies solely on the signs of the differences, ignoring their magnitude. In contrast, the t -test directly incorporates the magnitude of the density ratio differences. This approach leverages the theoretical property established in Lemma 2, which states that when X causes Y , the density ratio diverges at one end and vanishes at the other. This behavior leads to large consecutive differences, which are more effectively detected by the t -test.

Algorithm 1: Density Ratio-based Causal Discovery (DRCD)

Input: D : Dataset consisting of continuous variable X and discrete variable Y , α : Significance level, n_{points} : Number of grid points.

Output: Estimated causal relationship between X and Y

```

1 function DRCD( $D, \alpha, n_{\text{points}}$ )
2   // Step 1: Testing for causal existence.
3    $c_s, c_t \leftarrow$  the two distinct values of  $Y$  with the largest frequencies
4    $p_{\text{KS}} \leftarrow$  two-sample Kolmogorov–Smirnov test  $p$ -value comparing  $\{x \in X|Y = c_s\}$  and  $\{x \in X|Y = c_t\}$ 
5   if  $p_{\text{KS}} > \alpha$  then
6     return “No causal relationship between  $X$  and  $Y$ ” // Conditional distributions are statistically indistinguishable.
7   // Step 2: Density ratio estimation and determining the valid domain for evaluation.
8    $G_{c_s, c_t}(x) \leftarrow$  estimate of the density ratio  $\frac{p_{X|Y}(x|c_t)}{p_{X|Y}(x|c_s)}$  using RuLSIF [34]
9    $x_{\min} \leftarrow \min\{x \in X|Y = c_s\}, \min\{x \in X|Y = c_t\}$ 
10   $x_{\max} \leftarrow \max\{x \in X|Y = c_s\}, \max\{x \in X|Y = c_t\}$ 
11  // Step 3: Evaluating monotonicity to determine causal direction.
12   $\mathcal{X} \leftarrow (x_k)_{k=1}^{n_{\text{points}}}$  where  $x_k$  are equidistant points in  $[x_{\min}, x_{\max}]$ 
13   $\mathcal{D} \leftarrow (G_{c_s, c_t}(x_k) - G_{c_s, c_t}(x_{k-1}))_{k=2}^{n_{\text{points}}}$ 
14   $p_t \leftarrow$   $p$ -value from one-sample  $t$ -test on  $\mathcal{D}$  with null hypothesis that the mean is 0
15  if  $p_t < \alpha$  then
16    return “ $X$  causes  $Y$ ” //  $G_{c_s, c_t}(x)$  exhibits a monotonic pattern.
17  else
18    return “ $Y$  causes  $X$ ” //  $G_{c_s, c_t}(x)$  exhibits a non-monotonic pattern.

```

6 Experiments

In this section, we present comparative experiments using both synthetic and real-world datasets. The methods compared in our evaluation include LiM [35], MIC [32], CRACK [16], HCM [13], and GSF [8]. Detailed experimental settings are provided in Appendix C.

6.1 Experiments with Synthetic Data

We conducted experiments using synthetic data generated under three causal scenarios. In all cases, we use independent noise variables ξ_1 to ξ_7 , sampled from a mixture distribution described below, to construct X and Y .

Case 1 (X causes Y): $X = \xi_1$, with $Y = 0$ if $aX + \xi_2 \geq b$ and $Y = 1$ otherwise.

Case 2 (Y causes X): $Y = N_1$, with $X = (1 - Y)\xi_3 + Y\xi_4$.

Table 1: Prediction accuracy (%) of causal discovery methods on synthetic datasets with 95% confidence intervals.

Method	No Causation	$X \rightarrow Y$	$Y \rightarrow X$	Overall
DRCD	95.3% (93.9–96.6%)	85.8% (83.6–87.9%)	85.0% (82.8–87.2%)	88.7% (87.6–89.8%)
MIC	95.3% (93.9–96.6%)	72.3% (69.5–75.1%)	1.8% (1.0–2.7%)	56.5% (54.7–58.2%)
LiM	4.5% (3.3–5.8%)	0.0% (0.0–0.0%)	44.8% (41.7–47.9%)	16.4% (15.1–17.8%)
CRACK	0.0% (0.0–0.0%)	18.4% (16.0–20.8%)	100.0% (100.0–100.0%)	39.5% (37.7–41.2%)
HCM	97.9% (97.0–98.7%)	0.0% (0.0–0.0%)	45.0% (41.9–48.1%)	47.6% (45.8–49.4%)
GSF	100.0% (100.0–100.0%)	44.0% (40.9–47.1%)	0.3% (0.0–0.7%)	48.1% (46.3–49.9%)

Case 3 (No causal relationship): $X = \xi_5$ and $Y = N_2$.

In Section 3, we assumed that ξ_3 and ξ_4 satisfy the TSRV condition, while this was not required for ξ_1 , ξ_2 , and ξ_5 . However, since the TSRV condition is commonly observed in practice, we model all ξ_i as being drawn from the same mixture distribution $p_{\text{TSRV}}(x) = \sum_{i=1}^3 \pi_i f_i(x)$, where $\pi \sim \text{Dirichlet}(\mathbf{1})$. The component distributions are: Gaussian $f_1(x) = \mathcal{N}(x; \mu_1, \sigma_1^2)$, Student’s t -distribution $f_2(x) = t(x; \nu = 1)$, and Laplace $f_3(x) = \text{Laplace}(x; \mu_3, b_3)$. The parameters are sampled from uniform distributions: $\mu_1, \mu_3 \sim \mathcal{U}(-3, 3)$ and $\sigma_1, b_3 \sim \mathcal{U}(0.5, 3)$. The binary variables N_1 and N_2 are defined as $N_j = 1$ if $\xi_{j+5} < 0$ and $N_j = 0$ otherwise, for $j \in \{1, 2\}$. Both ξ_6 and ξ_7 are also drawn from the TSRV mixture distribution defined above. For each case, we generated 1000 datasets, with each dataset containing 1000 samples, and conducted experiments on all datasets.

Table 1 presents the prediction accuracy results. The columns represent the accuracy for Cases 1–3 and overall performance. Values in parentheses indicate 95% confidence intervals calculated using the percentile point function of the binomial distribution. DRCD consistently maintains high accuracy (>80%) across all causal scenarios, unlike other methods.

6.2 Experiments using real-world data

We conducted comparative experiments using the UCI Heart Disease dataset [9]. For each method, we inferred causal relationships between all numerical-categorical variable pairs, regardless of their multivariate analysis capabilities. The dataset contains several variables without missing values, including numerical variables (**age**: patient age, **chol**: serum cholesterol, **oldpeak**: ST depression, **thalach**: maximum heart rate, **trestbps**: resting blood pressure) and categorical variables (**cp**: chest pain type, **exang**: exercise-induced angina, **fbs**: fasting blood sugar status, **num**: heart disease diagnosis, **restecg**: resting ECG results, **sex**: gender, **slope**: ST segment slope).

Figure 2 displays the inferred causal relationships for each method. The nodes in the upper row of the graphs are numerical variables, and the nodes in the lower row are categorical variables. To make the direction of edges easier to understand, edges pointing from the upper row to the lower row are represented by black solid lines, while edges pointing from the lower row to the upper row are represented by blue dashed lines. While there is no definitive ground truth for these causal relationships, certain constraints exist. Variables **age** and **sex** can only be causes and not effects, and **num** is a diagnostic result that cannot be a cause of other variables. Evaluating methods against these constraints, only DRCD satisfies all the conditions that **age** and **sex** are not the results of other variables, and **num** is not the cause of other variables. In DRCD, **sex** is only connected to **chol**, and this causal relationship is consistent with the existing research findings [11, 19, 31].

7 Limitations

Our approach relies on three key assumptions: (1) absence of unobserved confounders, (2) the TSRV condition, and (3) a condition on the asymptotic behavior of log conditional densities (Equation 5), which is particularly relevant when the discrete variable Y causes the continuous variable X . Specifically, Equation 5 requires that $\log p_{X|Y}(x|c_i)$ and $\log p_{X|Y}(x|c_j)$ do not become asymptotically indistinguishable as $|x| \rightarrow \infty$; that is, their difference $h(x)$ must not

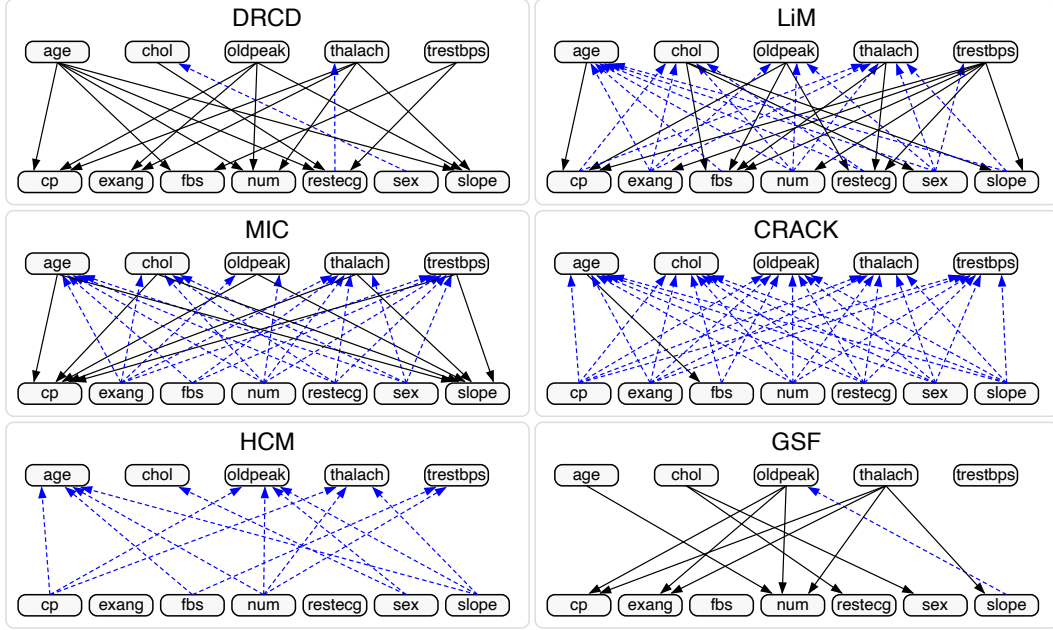


Figure 2: Inferred causal links between numerical (top) and categorical (bottom) variables in the UCI Heart Disease dataset. Methods were applied to all numerical-categorical pairs.

become negligible relative to both $\log p_{X|Y}(x|c_i)$ and $\log p_{X|Y}(x|c_j)$ in the tails. The scope of our method is limited to settings where these assumptions approximately hold.

Although each of the three assumptions is unverifiable, they differ in their consequences. The first assumption, which has implications for inference regardless of the true causal relationships, is unavoidable for all methods applicable to bivariate mixed data. In contrast, the second and third assumptions are relevant only in the $Y \rightarrow X$ case. In such settings, incorrect inference may occur if the density ratio $p_{X|Y}(x|c_i)/p_{X|Y}(x|c_j)$ exhibits monotonicity, which is a property rarely found between unrelated conditional distributions in general.

For the third assumption, violation of Equation 5 indicates that the dominant (i.e., leading-order) terms of $\log p_{X|Y}(x|c_i)$ and $\log p_{X|Y}(x|c_j)$ cancel each other out. In such cases, our model does not constrain the difference $h(x) = \log p_{X|Y}(x|c_i) - \log p_{X|Y}(x|c_j)$ to have similar behavior in the tails. Among representative distributions, location-shifted Gaussian or Laplace distributions with identical scale yield monotonic differences between their log-densities (See Appendix D.1 for detailed proofs). In the Gaussian case, $h(x)$ is linear, while in the Laplace case, it is piecewise linear: both resulting in monotonic behavior of density ratios $\exp(h(x)) = p_{X|Y}(x|c_i)/p_{X|Y}(x|c_j)$. Therefore, caution is necessary for cases where $p_{X|Y}(x|c_i)$ and $p_{X|Y}(x|c_j)$ arise from such distributions. In practice, these cases can be detected using variance comparisons and goodness-of-fit tests (See Appendix D.2 for an algorithm). When such patterns are observed, alternative causal discovery methods specifically designed for location-shifted models, such as LiM [35] or MIC [32], are recommended (see Section 2).

8 Conclusion

We proposed a novel method, DRCD, for causal discovery from bivariate mixed data. Our approach is grounded in a key theoretical insight: the monotonicity of the conditional density ratio enables identification of causal direction without relying on restrictive distributional assumptions or normalization heuristics. Future work includes (1) extending the theoretical framework to multivariate settings, (2) accommodating potential confounding variables, (3) developing techniques to identify when datasets violate our assumptions, and (4) integrating monotonicity-based criteria with other causal discovery methods. Overall, our findings provide a foundation for advancing principled causal discovery in heterogeneous data settings.

References

- [1] Ruichu Cai, Jie Qiao, Kun Zhang, Zhenjie Zhang, and Zhifeng Hao. Causal discovery from discrete data using hidden compact representation. In S. Bengio, H. Wallach, H. Larochelle, K. Grauman, N. Cesa-Bianchi, and R. Garnett, editors, *Advances in Neural Information Processing Systems*, volume 31. Curran Associates, Inc., 2018.
- [2] Ruichu Cai, Jie Qiao, Kun Zhang, Zhenjie Zhang, and Zhifeng Hao. Causal discovery with cascade nonlinear additive noise model. In *Proceedings of the Twenty-Eighth International Joint Conference on Artificial Intelligence, IJCAI-19*, pages 1609–1615. International Joint Conferences on Artificial Intelligence Organization, 7 2019.
- [3] David Maxwell Chickering. Optimal structure identification with greedy search. *Journal of Machine Learning Research*, 3(Nov):507–554, 2002.
- [4] Ruifei Cui, Perry Groot, and Tom Heskes. Copula pc algorithm for causal discovery from mixed data. In Paolo Frasconi, Niels Landwehr, Giuseppe Manco, and Jilles Vreeken, editors, *Machine Learning and Knowledge Discovery in Databases*, pages 377–392, Cham, 2016. Springer International Publishing.
- [5] Xiaoyu Ge, Vineet K Raghu, Panos K Chrysanthis, and Panayiotis V Benos. Causalmgm: an interactive web-based causal discovery tool. *Nucleic Acids Research*, 48(W1):W597–W602, 05 2020.
- [6] Clark Glymour, Kun Zhang, and Peter Spirtes. Review of causal discovery methods based on graphical models. *Frontiers in Genetics*, Volume 10 - 2019, 2019.
- [7] Patrik O. Hoyer, Dominik Janzing, Joris M. Mooij, Jonas Peters, and Bernhard Schölkopf. Nonlinear causal discovery with additive noise models. In D. Koller, D. Schuurmans, Y. Bengio, and L. Bottou, editors, *Advances in Neural Information Processing Systems 21*, pages 689–696. Curran Associates, Inc., 2009.
- [8] Biwei Huang, Kun Zhang, Yizhu Lin, Bernhard Schölkopf, and Clark Glymour. Generalized score functions for causal discovery. In *Proceedings of the 24th ACM SIGKDD International Conference on Knowledge Discovery & Data Mining, KDD ’18*, pages 1551–1560, New York, NY, USA, 2018. Association for Computing Machinery.
- [9] Steinbrunn William Pfisterer Matthias Janosi, Andras and Robert Detrano. Heart Disease. UCI Machine Learning Repository, 1989. DOI: <https://doi.org/10.24432/C52P4X>.
- [10] Christoph Käding and Jakob Runge. Distinguishing cause and effect in bivariate structural causal models: A systematic investigation. *Journal of Machine Learning Research*, 24(278):1–144, 2023.
- [11] Kalypso Karastergiou, Steven R. Smith, Andrew S. Greenberg, and Susan K. Fried. Sex differences in human adipose tissues –the biology of pear shape. *Biology of Sex Differences*, 3(1):13, 2012.
- [12] Maurice G Kendall. *Rank correlation methods*. Charles Griffin & Co. Ltd., London, 1948.
- [13] Yan Li, Rui Xia, Chunchen Liu, and Liang Sun. A hybrid causal structure learning algorithm for mixed-type data. *Proceedings of the AAAI Conference on Artificial Intelligence*, 36(7):7435–7443, Jun. 2022.
- [14] Henry B. Mann. Nonparametric tests against trend. *Econometrica*, 13(3):245–259, 1945.
- [15] Alexander Marx and Jilles Vreeken. Telling Cause from Effect Using MDL-Based Local and Global Regression . In *2017 IEEE International Conference on Data Mining (ICDM)*, pages 307–316, Los Alamitos, CA, USA, November 2017. IEEE Computer Society.

- [16] Alexander Marx and Jilles Vreeken. Causal inference on multivariate and mixed-type data. In Michele Berlingerio, Francesco Bonchi, Thomas Gärtner, Neil Hurley, and Georgiana Ifrim, editors, *Machine Learning and Knowledge Discovery in Databases*, pages 655–671, Cham, 2019. Springer International Publishing.
- [17] Alexander Marx and Jilles Vreeken. Identifiability of cause and effect using regularized regression. In *Proceedings of the 25th ACM SIGKDD International Conference on Knowledge Discovery & Data Mining*, KDD ’19, pages 852–861, New York, NY, USA, 2019. Association for Computing Machinery.
- [18] Joris M. Mooij, Jonas Peters, Dominik Janzing, Jakob Zscheischler, and Bernhard Schölkopf. Distinguishing cause from effect using observational data: Methods and benchmarks. *Journal of Machine Learning Research*, 17(32):1–102, 2016.
- [19] Brian T. Palmisano, Lin Zhu, Robert H. Eckel, and John M. Stafford. Sex differences in lipid and lipoprotein metabolism. *Molecular Metabolism*, 15:45–55, 2018. Sex and Gender Differences in Metabolism (2018).
- [20] Judea Pearl. *Causality: models, reasoning and inference*. Cambridge University Press, 2000.
- [21] Jonas Peters, Dominik Janzing, and Bernhard Schölkopf. Identifying cause and effect on discrete data using additive noise models. In Yee Whye Teh and Mike Titterton, editors, *Proceedings of the Thirteenth International Conference on Artificial Intelligence and Statistics*, volume 9 of *Proceedings of Machine Learning Research*, pages 597–604, Chia Laguna Resort, Sardinia, Italy, 13–15 May 2010. PMLR.
- [22] Jonas Peters, Joris M. Mooij, Dominik Janzing, and Bernhard Schölkopf. Causal discovery with continuous additive noise models. *The Journal of Machine Learning Research*, 15(1):2009–2053, 2014.
- [23] Eleni Sgouritsa, Dominik Janzing, Philipp Hennig, and Bernhard Schölkopf. Inference of Cause and Effect with Unsupervised Inverse Regression. In Guy Lebanon and S. V. N. Vishwanathan, editors, *Proceedings of the Eighteenth International Conference on Artificial Intelligence and Statistics*, volume 38 of *Proceedings of Machine Learning Research*, pages 847–855, San Diego, California, USA, 09–12 May 2015. PMLR.
- [24] Shohei Shimizu, Patrik O. Hoyer, Aapo Hyvärinen, and Antti Kerminen. A linear non-Gaussian acyclic model for causal discovery. *Journal of Machine Learning Research*, 7(Oct):2003–2030, 2006.
- [25] Shohei Shimizu, Takanori Inazumi, Yasuhiro Sogawa, Aapo Hyvärinen, Yoshinobu Kawahara, Takashi Washio, Patrik O. Hoyer, and Kenneth Bollen. DirectLiNGAM: a direct method for learning a linear non-Gaussian structural equation model. *Journal of Machine Learning Research*, 12(Apr):1225–1248, 2011.
- [26] Peter Spirtes and Clark Glymour. An algorithm for fast recovery of sparse causal graphs. *Social Science Computer Review*, 9(1):62–72, 1991.
- [27] Peter Spirtes, Clark N Glymour, Richard Scheines, David Heckerman, Christopher Meek, Gregory Cooper, and Thomas Richardson. *Causation, prediction, and search*. MIT press, 2000.
- [28] Peter Spirtes, Christopher Meek, and Thomas Richardson. Causal discovery in the presence of latent variables and selection bias. In Gregory Floyd Cooper and Clark N Glymour, editors, *Computation, Causality, and Discovery*, pages 211–252. AAAI Press, 1999.
- [29] Natasa Tagasovska, Valérie Chavez-Demoulin, and Thibault Vatter. Distinguishing cause from effect using quantiles: Bivariate quantile causal discovery. In Hal Daumé III and Aarti Singh, editors, *Proceedings of the 37th International Conference on Machine Learning*, volume 119 of *Proceedings of Machine Learning Research*, pages 9311–9323. PMLR, 13–18 Jul 2020.

- [30] Michail Tsagris, Giorgos Borboudakis, Vincenzo Lagani, and Ioannis Tsamardinos. Constraint-based causal discovery with mixed data. *International Journal of Data Science and Analytics*, 6(1):19–30, 2018.
- [31] Xuewen Wang, Faidon Magkos, and Bettina Mittendorfer. Sex differences in lipid and lipoprotein metabolism: It’s not just about sex hormones. *The Journal of Clinical Endocrinology & Metabolism*, 96(4):885–893, 04 2011.
- [32] Wei Wenjuan, Feng Lu, and Liu Chunchen. Mixed causal structure discovery with application to prescriptive pricing. In *Proceedings of the Twenty-Seventh International Joint Conference on Artificial Intelligence, IJCAI-18*, pages 5126–5134. International Joint Conferences on Artificial Intelligence Organization, 7 2018.
- [33] Sascha Xu, Osman A Mian, Alexander Marx, and Jilles Vreeken. Inferring cause and effect in the presence of heteroscedastic noise. In Kamalika Chaudhuri, Stefanie Jegelka, Le Song, Csaba Szepesvari, Gang Niu, and Sivan Sabato, editors, *Proceedings of the 39th International Conference on Machine Learning*, volume 162 of *Proceedings of Machine Learning Research*, pages 24615–24630. PMLR, 17–23 Jul 2022.
- [34] Makoto Yamada, Taiji Suzuki, Takafumi Kanamori, Hirotaka Hachiya, and Masashi Sugiyama. Relative density-ratio estimation for robust distribution comparison. In J. Shawe-Taylor, R. Zemel, P. Bartlett, F. Pereira, and K.Q. Weinberger, editors, *Advances in Neural Information Processing Systems*, volume 24. Curran Associates, Inc., 2011.
- [35] Yan Zeng, Shohei Shimizu, Hidetoshi Matsui, and Fuchun Sun. Causal discovery for linear mixed data. In Bernhard Schölkopf, Caroline Uhler, and Kun Zhang, editors, *Proceedings of the First Conference on Causal Learning and Reasoning*, volume 177 of *Proceedings of Machine Learning Research*, pages 994–1009. PMLR, 11–13 Apr 2022.

Appendices: **“Density Ratio-based Causal Discovery** **from Bivariate Continuous-Discrete Data”**

Contents

A	Proofs	14
• A.1	Proof of Lemma 1	14
• A.2	Proof of Lemma 2	16
• A.3	Proof of Lemma 3	17
B	Illustrative example settings	19
C	Details of the experiments	20
• C.1	Code availability	20
• C.2	Code packages	20
• C.3	Experimental settings	20
• C.4	Computational resources	21
D	Failure cases and detection methods	21
• D.1	Monotonicity in Gaussian and Laplace cases	21
• D.2	Detection of Gaussian and Laplace cases	22

A Proofs

A.1 The proof of Lemma 1

Lemma 1: Let X_1, X_2, \dots, X_n be random variables that all satisfy the TSRV condition. If the probability density function of a random variable X is given by

$$P_X(x) = \sum_{i=1}^n \omega_i P_{X_i}(x),$$

with $\omega_i > 0$ and $\sum_{i=1}^n \omega_i = 1$, then X also satisfies the TSRV condition.

Proof. Define the density functions as:

$$\begin{aligned} P_X(x) &= \exp(f(x)), \\ P_{X_i}(x) &= \exp(g_i(x)) \quad \text{for } i = 1, 2, \dots, n. \end{aligned}$$

Then,

$$e^{f(x)} = \sum_{i=1}^n \omega_i e^{g_i(x)},$$

so

$$f(x) = \log \left(\sum_{i=1}^n \omega_i e^{g_i(x)} \right).$$

To prove that X satisfies the TSRV condition, we need to show:

$$\lim_{x \rightarrow \pm\infty} f(x) = -\infty, \tag{10}$$

$$\lim_{x \rightarrow \infty} \frac{f(x)}{f(-x)} = 1. \tag{11}$$

Proof of (10). Since $g_i(x) \rightarrow -\infty$ as $x \rightarrow \pm\infty$ for all $i = 1, 2, \dots, n$, we have

$$\sum_{i=1}^n \omega_i e^{g_i(x)} \rightarrow 0.$$

Hence,

$$f(x) = \log \left(\sum_{i=1}^n \omega_i e^{g_i(x)} \right) \rightarrow -\infty,$$

as $x \rightarrow \pm\infty$.

Proof of (11). Define:

$$M(x) = \max\{g_1(x), g_2(x), \dots, g_n(x)\}. \tag{12}$$

We claim:

$$\lim_{x \rightarrow \infty} \frac{M(x)}{M(-x)} = 1. \tag{13}$$

Lower Bound. For each $i = 1, 2, \dots, n$, let $\epsilon_i(x) \rightarrow 0$ such that $g_i(x) = g_i(-x)(1 + \epsilon_i(x))$.

Let i^* be such that $M(x) = g_{i^*}(x)$, then:

$$g_{i^*}(x) = g_{i^*}(-x)(1 + \epsilon_{i^*}(x))$$

so

$$g_{i^*}(-x) = \frac{g_{i^*}(x)}{1 + \epsilon_{i^*}(x)} = \frac{M(x)}{1 + \epsilon_{i^*}(x)}$$

Since

$$M(-x) = \max\{g_1(-x), g_2(-x), \dots, g_n(-x)\} \geq g_{i^*}(-x)$$

We obtain

$$M(-x) \geq g_{i^*}(-x) = \frac{M(x)}{1 + \epsilon_{i^*}(x)}$$

According to the TSRV condition, both $\lim_{x \rightarrow \pm\infty} g_i(x) = -\infty$ and $\lim_{x \rightarrow \infty} \frac{g_i(x)}{g_i(-x)} = 1$ hold for each $i \in \{1, 2, \dots, n\}$. Therefore, there exists a positive constant τ such that

$$\forall i \in \{1, 2, \dots, n\}, \forall x \in (-\infty, -\tau) \cup (\tau, \infty), \quad g_i(x) < 0 \quad \text{and} \quad 1 + \epsilon_{i^*}(x) > 0. \quad (14)$$

Since $g_i(x) < 0$ for all i when $|x| > \tau$, it follows that $g_i(-x) < 0$ for all i in this region. Consequently, $M(-x) = \max\{g_1(-x), g_2(-x), \dots, g_n(-x)\} < 0$ also holds in this region. Then, we have

$$\frac{M(x)}{M(-x)} \geq 1 + \epsilon_{i^*}(x).$$

So:

$$\frac{M(x)}{M(-x)} \geq 1 + \epsilon_{i^*}(x) \quad \Rightarrow \quad \liminf_{x \rightarrow \infty} \frac{M(x)}{M(-x)} \geq 1. \quad (15)$$

Upper Bound. Let j^* be such that $M(-x) = g_{j^*}(-x)$, and define $\delta_{j^*}(x) \rightarrow 0$ with:

$$g_{j^*}(-x) = g_{j^*}(x)(1 + \delta_{j^*}(x)).$$

so

$$g_{j^*}(x) = \frac{g_{j^*}(-x)}{1 + \delta_{j^*}(x)} = \frac{M(-x)}{1 + \delta_{j^*}(x)}$$

Since

$$M(x) = \max\{g_1(x), g_2(x), \dots, g_n(x)\} \geq g_{j^*}(x)$$

We obtain

$$M(x) \geq g_{j^*}(x) = \frac{M(-x)}{1 + \delta_{j^*}(x)}$$

In the region $(-\infty, -\tau) \cup (\tau, \infty)$, $M(-x) < 0$ holds, and we have

$$\frac{M(x)}{M(-x)} \leq \frac{1}{1 + \delta_{j^*}(x)}$$

So:

$$\frac{M(x)}{M(-x)} \leq \frac{1}{1 + \delta_{j^*}(x)} \quad \Rightarrow \quad \limsup_{x \rightarrow \infty} \frac{M(x)}{M(-x)} \leq 1.$$

Thus:

$$\lim_{x \rightarrow \infty} \frac{M(x)}{M(-x)} = 1.$$

Now we analyze:

$$\begin{aligned} \frac{f(x)}{f(-x)} &= \frac{\log(\sum_{i=1}^n \omega_i e^{g_i(x)})}{\log(\sum_{i=1}^n \omega_i e^{g_i(-x)})} \\ &= \frac{M(x) + \log(\sum_{i=1}^n \omega_i e^{g_i(x) - M(x)})}{M(-x) + \log(\sum_{i=1}^n \omega_i e^{g_i(-x) - M(-x)})}. \end{aligned} \quad (16)$$

Since $g_i(x) - M(x) \leq 0$ for all i , we know the logarithmic terms are bounded:

$$\log \left(\sum_{i=1}^n \omega_i e^{g_i(x) - M(x)} \right) = O(1),$$

and similarly in the denominator. Therefore,

$$\frac{f(x)}{f(-x)} = \frac{M(x) + O(1)}{M(-x) + O(1)} \rightarrow 1. \quad (17)$$

This completes the proof that X satisfies the TSRV property. \square

A.2 The proof of Lemma 2

Lemma 2: Assume that (X, Y) are generated according to the model described in Section 3.1 with the causal direction $X \rightarrow Y$. Then, for any distinct outcomes c_s and c_t of Y , the function $G_{c_s, c_t}(x)$ is monotonic in x . Additionally, $G_{c_s, c_t}(x)$ satisfies either $\lim_{x \rightarrow -\infty} G_{c_s, c_t}(x) = \infty$ and $\lim_{x \rightarrow \infty} G_{c_s, c_t}(x) = 0$, or $\lim_{x \rightarrow -\infty} G_{c_s, c_t}(x) = 0$ and $\lim_{x \rightarrow \infty} G_{c_s, c_t}(x) = \infty$.

Proof. Recall that in our model (Section 3.1), the output Y is generated by a binary decision tree. Hence, for any two distinct outcomes c_s and c_t , there exists a decision node, say indexed by i , at which the tree branches so that the observations with $Y = c_s$ and $Y = c_t$ are separated. More precisely, either

$$(X = x) \wedge (a_i x + N_{Y,i} < b_i) \wedge (Y \in \{c_s, c_t\}) \iff (X = x) \wedge (Y = c_s), \quad (18)$$

and

$$(X = x) \wedge (a_i x + N_{Y,i} \geq b_i) \wedge (Y \in \{c_s, c_t\}) \iff (X = x) \wedge (Y = c_t). \quad (19)$$

or

$$(X = x) \wedge (a_i x + N_{Y,i} \geq b_i) \wedge (Y \in \{c_s, c_t\}) \iff (X = x) \wedge (Y = c_s), \quad (20)$$

and

$$(X = x) \wedge (a_i x + N_{Y,i} < b_i) \wedge (Y \in \{c_s, c_t\}) \iff (X = x) \wedge (Y = c_t). \quad (21)$$

Without loss of generality, assume that (18) and (19) hold. Then, we have

$$P(Y = c_s \mid X = x, Y \in \{c_s, c_t\}) = P(a_i x + N_{Y,i} < b_i \mid X = x, Y \in \{c_s, c_t\}), \quad (22)$$

and

$$\begin{aligned} P(Y = c_t \mid X = x, Y \in \{c_s, c_t\}) &= 1 - P(Y = c_s \mid X = x, Y \in \{c_s, c_t\}) \\ &= 1 - P(a_i x + N_{Y,i} < b_i \mid X = x, Y \in \{c_s, c_t\}). \end{aligned} \quad (23)$$

Using Bayes' rule, the conditional density for X given $Y = c_s$ can be written as

$$\begin{aligned} p_{X|Y=c_s}(x) &= \frac{P(Y = c_s \mid X = x)p_X(x)}{p_Y(c_s)} \\ &= \frac{P(Y = c_s \mid X = x, Y \in \{c_s, c_t\})p_X(x)P(Y \in \{c_s, c_t\})}{p_Y(c_s)} \\ &= \frac{P(Y = c_s \mid X = x, Y \in \{c_s, c_t\})p_X(x)(p_Y(c_s) + p_Y(c_t))}{p_Y(c_s)} \\ &= \frac{P(a_i x + N_{Y,i} < b_i \mid X = x, Y \in \{c_s, c_t\})p_X(x)(p_Y(c_s) + p_Y(c_t))}{p_Y(c_s)}. \end{aligned} \quad (24)$$

The conditional density for X given $Y = c_t$ can be written as

$$\begin{aligned}
p_{X|Y=c_t}(x) &= \frac{P(Y = c_t | X = x)p_X(x)}{p_Y(c_t)} \\
&= \frac{P(Y = c_t | X = x, Y \in \{c_s, c_t\})p_X(x)(p_Y(c_s) + p_Y(c_t))}{p_Y(c_t)} \\
&= \frac{\left(1 - P(a_i x + N_{Y,i} < b_i | X = x, Y \in \{c_s, c_t\})\right)p_X(x)(p_Y(c_s) + p_Y(c_t))}{p_Y(c_t)}.
\end{aligned} \tag{25}$$

Since $N_{Y,i}$ is independent of X , we have

$$\begin{aligned}
P(a_i x + N_{Y,i} < b_i | X = x, Y \in \{c_s, c_t\}) &= \int_{-\infty}^{b_i - a_i x} p_{N_{Y,i}|Y \in \{c_s, c_t\}}(u) du \\
&= F_{N_{Y,i}|Y \in \{c_s, c_t\}}(b_i - a_i x) \\
&\triangleq H(b_i - a_i x).
\end{aligned} \tag{26}$$

$H(b_i - a_i x)$ is the cumulative distribution function of $N_{Y,i}$ given $Y \in \{c_s, c_t\}$ (note that $H(u)$ satisfies $\lim_{u \rightarrow \infty} H(u) = 1$ and $\lim_{u \rightarrow -\infty} H(u) = 0$). Then, we obtain

$$p_{X|Y=c_s}(x) = \frac{H(b_i - a_i x)}{p_Y(c_s)} p_X(x)(p_Y(c_s) + p_Y(c_t)). \tag{27}$$

Similarly, the conditional density for X given $Y = c_t$ is

$$p_{X|Y=c_t}(x) = \frac{1 - H(b_i - a_i x)}{p_Y(c_t)} p_X(x)(p_Y(c_s) + p_Y(c_t)). \tag{28}$$

We let A denote a constant as $A = \frac{P(Y=c_s)}{P(Y=c_t)}$. Combining (27) and (28), the density ratio becomes

$$G_{c_s, c_t}(x) = \frac{p_{X|Y=c_t}(x)}{p_{X|Y=c_s}(x)} = A \cdot \frac{1 - H(b_i - a_i x)}{H(b_i - a_i x)}. \tag{29}$$

Since $H(b_i - a_i x)$ is monotonic in x (because H is a CDF and $b_i - a_i x$ is affine in x), it follows that $G_{c_s, c_t}(x)$ is monotonic in x .

Additionally, because $H(u)$ is a cumulative distribution function, we have

$$\lim_{x \rightarrow -\infty} H(b_i - a_i x) = \begin{cases} 1 & \text{if } a_i > 0, \\ 0 & \text{if } a_i < 0, \end{cases} \quad \text{and} \quad \lim_{x \rightarrow \infty} H(b_i - a_i x) = \begin{cases} 0 & \text{if } a_i > 0, \\ 1 & \text{if } a_i < 0. \end{cases} \tag{30}$$

Therefore, depending on the sign of a_i , the ratio $\frac{1 - H(b_i - a_i x)}{H(b_i - a_i x)}$ diverges in one direction and vanishes in the other. As a result, $G_{c_s, c_t}(x)$ satisfies either

$$\lim_{x \rightarrow -\infty} G_{c_s, c_t}(x) = \infty \quad \text{and} \quad \lim_{x \rightarrow \infty} G_{c_s, c_t}(x) = 0, \tag{31}$$

or

$$\lim_{x \rightarrow -\infty} G_{c_s, c_t}(x) = 0 \quad \text{and} \quad \lim_{x \rightarrow \infty} G_{c_s, c_t}(x) = \infty. \tag{32}$$

This completes the proof. \square

A.3 The proof of Lemma 3

Lemma 3: Suppose that (X, Y) are generated according to the model described in Section 3.2 with the causal direction $Y \rightarrow X$. Then, for any distinct c_s and c_t of Y , the function $G_{c_s, c_t}(x)$ is non-monotonic with respect to x . Additionally, $G_{c_s, c_t}(x)$ satisfies either $\lim_{x \rightarrow \pm\infty} G_{c_s, c_t}(x) = 0$ or $\lim_{x \rightarrow \pm\infty} G_{c_s, c_t}(x) = \infty$.

Proof. From the assumption of Lemma 3, we obtain

$$\begin{aligned}
G_{c_s, c_t}(x) &= \frac{P(X = x|Y = c_t)}{P(X = x|Y = c_s)} \\
&= \frac{P_{N_{X,t}}(N_{X,t} = x)}{P_{N_{X,s}}(N_{X,s} = x)} \\
&= \frac{e^{g_t(x)}}{e^{g_s(x)}} \\
&= \exp(g_t(x) - g_s(x)).
\end{aligned} \tag{33}$$

Since X conditioned on Y satisfies the TSRV condition, we have

$$\lim_{x \rightarrow \infty} \frac{g_t(x)}{g_t(-x)} = 1 \quad \text{and} \quad \lim_{x \rightarrow \infty} \frac{g_s(x)}{g_s(-x)} = 1. \tag{34}$$

If we define

$$L := \lim_{x \rightarrow \infty} \frac{g_t(x)}{g_s(x)}, \tag{35}$$

then by performing the substitution $u = -x$ we obtain

$$\lim_{x \rightarrow -\infty} \frac{g_t(x)}{g_s(x)} = \lim_{u \rightarrow \infty} \frac{g_t(-u)}{g_s(-u)} = \lim_{u \rightarrow \infty} \frac{g_t(u)/(1 + \epsilon_t(u))}{g_s(u)/(1 + \epsilon_s(u))} = L. \tag{36}$$

where $\epsilon_s(u)$ and $\epsilon_t(u)$ are defined as $\epsilon_s(u) = \frac{g_s(u)}{g_s(-u)} - 1$ and $\epsilon_t(u) = \frac{g_t(u)}{g_t(-u)} - 1$, respectively.

Since by the assumption defined in Section 3.2, $\lim_{x \rightarrow \infty} \frac{g_t(x)}{g_s(x)} \neq 1$ (and likewise for $x \rightarrow -\infty$), we must have $L \neq 1$; that is, either $L > 1$ or $L < 1$.

We may write

$$\exp(g_t(x) - g_s(x)) = \exp\left(g_s(x) \left\{ \frac{g_t(x)}{g_s(x)} - 1 \right\}\right). \tag{37}$$

We now consider the two cases.

Case 1: $L > 1$.

In this case, as $x \rightarrow \infty$ (and similarly as $x \rightarrow -\infty$) we have

$$\frac{g_t(x)}{g_s(x)} \rightarrow L > 1, \tag{38}$$

so that for all sufficiently large $|x|$,

$$\frac{g_t(x)}{g_s(x)} - 1 > 0. \tag{39}$$

According to the TSRV condition, $g_s(x) \rightarrow -\infty$ as $|x| \rightarrow \infty$. Then, we deduce that

$$g_s(x) \left\{ \frac{g_t(x)}{g_s(x)} - 1 \right\} \rightarrow -\infty. \tag{40}$$

Thus,

$$\exp(g_t(x) - g_s(x)) \rightarrow \exp(-\infty) = 0. \tag{41}$$

Then, we have

$$\lim_{x \rightarrow \infty} \exp(g_t(x) - g_s(x)) = 0 \quad \text{and} \quad \lim_{x \rightarrow -\infty} \exp(g_t(x) - g_s(x)) = 0. \tag{42}$$

Case 2: $L < 1$.

In this case, as $x \rightarrow \infty$ (and similarly as $x \rightarrow -\infty$) we have

$$\frac{g_t(x)}{g_s(x)} \rightarrow L < 1, \tag{43}$$

so that for all sufficiently large $|x|$,

$$\frac{g_t(x)}{g_s(x)} - 1 < 0. \quad (44)$$

According to the TSRV condition, $g_s(x) \rightarrow -\infty$ as $|x| \rightarrow \infty$. Then, we deduce that

$$g_s(x) \left\{ \frac{g_t(x)}{g_s(x)} - 1 \right\} \rightarrow +\infty. \quad (45)$$

Hence,

$$\exp(g_t(x) - g_s(x)) \rightarrow \exp(+\infty) = \infty. \quad (46)$$

Then, we have

$$\lim_{x \rightarrow \infty} \exp(g_t(x) - g_s(x)) = \infty \quad \text{and} \quad \lim_{x \rightarrow -\infty} \exp(g_t(x) - g_s(x)) = \infty. \quad (47)$$

Conclusion:

Thus, under the assumption stated in Lemma 3, either

$$\lim_{x \rightarrow \pm\infty} G_{c_s, c_t}(x) = 0 \quad \text{or} \quad \lim_{x \rightarrow \pm\infty} G_{c_s, c_t}(x) = \infty. \quad (48)$$

Since $G_{c_s, c_t}(x)$ is neither always 0 nor always ∞ for $x \in (-\infty, \infty)$, $G_{c_s, c_t}(x)$ is non-monotonic. This completes the proof. \square

B Illustrative example settings

This appendix explains the generative models used to produce the illustrative plots in Figure 1. Note that Gaussianity is assumed in these examples solely for illustrative purposes; our theoretical framework does not require such distributional assumptions.

Case 1: $X \rightarrow Y$

In this case, the continuous variable X causes the binary variable Y through a noisy threshold model. The structural equations are modeled as:

$$\begin{aligned} X &= \xi_X, \quad \xi_X \sim \mathcal{N}(0, 1), \\ Y &= \begin{cases} 1 & \text{if } X + \xi_Y > 0, \\ 0 & \text{otherwise,} \end{cases} \quad \xi_Y \sim \mathcal{N}(0, 1). \end{aligned}$$

Under this model, the distribution of X is:

$$P(X) = \mathcal{N}(X; 0, 1).$$

The conditional densities of X given Y are:

$$\begin{aligned} P(X | Y = 1) &= \frac{\Phi(X) \cdot \mathcal{N}(X; 0, 1)}{P(Y = 1)}, \\ P(X | Y = 0) &= \frac{(1 - \Phi(X)) \cdot \mathcal{N}(X; 0, 1)}{P(Y = 0)}, \end{aligned}$$

where $\Phi(\cdot)$ denotes the standard Gaussian cumulative distribution function, and $P(Y = 1) = P(Y = 0) = 0.5$ holds due to the symmetry of this model.

The resulting density ratio is:

$$\frac{P(X | Y = 1)}{P(X | Y = 0)} = \frac{\Phi(X)}{1 - \Phi(X)}.$$

Case 2: $Y \rightarrow X$

In this case, the binary variable Y causes the continuous variable X through a Gaussian mixture model. The structural equations are modeled as:

$$Y \sim \text{Bernoulli}(0.5),$$
$$X = \begin{cases} \xi_1, & \text{if } Y = 1, \\ \xi_2, & \text{if } Y = 0, \end{cases} \quad \xi_1 \sim \mathcal{N}(0.5, 0.25^2), \quad \xi_2 \sim \mathcal{N}(-0.5, 0.5^2).$$

The conditional distributions of X given Y are:

$$P(X | Y = 1) = \mathcal{N}(X; 0.5, 0.25^2), \quad P(X | Y = 0) = \mathcal{N}(X; -0.5, 0.5^2).$$

The distribution of X is:

$$P(X) = 0.5 \cdot \mathcal{N}(X; 0.5, 0.25^2) + 0.5 \cdot \mathcal{N}(X; -0.5, 0.5^2).$$

The density ratio is:

$$\frac{P(X | Y = 1)}{P(X | Y = 0)} = \frac{\mathcal{N}(X; 0.5, 0.25^2)}{\mathcal{N}(X; -0.5, 0.5^2)}.$$

C Details of the experiments

C.1 Code availability

The code for our proposed methodology and for conducting experiments with both synthetic and real-world data is available at <https://github.com/causal111/DRCD>.

C.2 Code packages

We utilized the following code packages for the experiments in our research:

- **LiM** (Causal discovery for linear mixed data) [35]
 - Repository: <https://github.com/cdt15/lingam>
 - Implementation language: Python
- **CRACK** (Classification and regression based packing of data) [16]
 - Repository: <https://eda.rg.cispa.io/prj/crack/>
 - Implementation language: C++
- **HCM** (A Hybrid Causal Structure Learning Algorithm for Mixed-type Data) [13]
 - Repository: <https://github.com/DAMO-DI-ML/AAAI2022-HCM>
 - Implementation language: Python
- **GSF** (Generalized Score Functions for Causal Discovery) [8]
 - Repository:
<https://github.com/Biwei-Huang/Generalized-Score-Functions-for-Causal-Discovery>
 - Implementation language: MATLAB
- **MIC** (Mixed causal structure discovery) [32]
 - Implementation language: Python
 - Note: We implemented this method ourselves in Python based on the original paper.

C.3 Experimental settings

For the parameter setting of the DRCD algorithm (refer to Algorithm 1), we set $\alpha = 0.05$ and $n_{\text{points}} = 1000$. For MIC, the penalty term was set to $\lambda = 0.1$. For other methods, we used the default parameter settings as provided in the code packages described in Appendix C.2.

C.4 Computational resources

All experiments were conducted on a MacBook Pro with the following specifications:

- CPU: Apple M3 Max chip (16 cores)
- Memory: 128 GB RAM
- Operating System: macOS Sonoma 14.4.1
- Programming Environment: Python 3.11.7

D Failure cases and detection methods

This appendix provides proofs of the monotonicity of density ratios for location-shifted Gaussian or Laplace distributions with identical scales, and presents an algorithm for detecting such cases.

D.1 Monotonicity in Gaussian and Laplace cases

Lemma 5 (Monotonicity in Gaussian cases). *Let $p_{X|Y}(x|c_i) = \mathcal{N}(x; \mu_i, \sigma^2)$ and $p_{X|Y}(x|c_j) = \mathcal{N}(x; \mu_j, \sigma^2)$ be two Gaussian distributions with means $\mu_i \neq \mu_j$ and identical variance σ^2 . Then their density ratio $G_{c_i, c_j}(x) = \frac{p_{X|Y}(x|c_i)}{p_{X|Y}(x|c_j)}$ is monotonic in x .*

Proof. For Gaussian distributions, we have:

$$\log p_{X|Y}(x|c_i) = -\frac{1}{2} \log(2\pi\sigma^2) - \frac{(x - \mu_i)^2}{2\sigma^2} \quad (49)$$

$$\log p_{X|Y}(x|c_j) = -\frac{1}{2} \log(2\pi\sigma^2) - \frac{(x - \mu_j)^2}{2\sigma^2} \quad (50)$$

The log-density difference is:

$$h(x) = \log p_{X|Y}(x|c_i) - \log p_{X|Y}(x|c_j) \quad (51)$$

$$= \frac{-(x - \mu_i)^2 + (x - \mu_j)^2}{2\sigma^2} \quad (52)$$

$$= \frac{(\mu_i - \mu_j)}{\sigma^2} \left(x - \frac{\mu_i + \mu_j}{2} \right) \quad (53)$$

This expression is linear in x with slope $\frac{\mu_i - \mu_j}{\sigma^2}$, which is non-zero when $\mu_i \neq \mu_j$. Therefore, $h(x)$ is monotonic, making the density ratio $\exp(h(x)) = G_{c_i, c_j}(x)$ monotonic as well. \square

Lemma 6 (Monotonicity in Laplace cases). *Let $p_{X|Y}(x|c_i) = \text{Laplace}(x; \mu_i, b)$ and $p_{X|Y}(x|c_j) = \text{Laplace}(x; \mu_j, b)$ be two Laplace distributions with means $\mu_i \neq \mu_j$ and identical scale parameter b . Then their density ratio $G_{c_i, c_j}(x) = \frac{p_{X|Y}(x|c_i)}{p_{X|Y}(x|c_j)}$ is monotonic.*

Proof. For Laplace distributions, we have:

$$\log p_{X|Y}(x|c_i) = -\log(2b) - \frac{|x - \mu_i|}{b} \quad (54)$$

$$\log p_{X|Y}(x|c_j) = -\log(2b) - \frac{|x - \mu_j|}{b} \quad (55)$$

The log-density difference is:

$$h(x) = \log p_{X|Y}(x|c_i) - \log p_{X|Y}(x|c_j) \quad (56)$$

$$= \frac{|x - \mu_j| - |x - \mu_i|}{b} \quad (57)$$

When $\mu_i < \mu_j$, $h(x)$ has the following piecewise form:

$$h(x) = \begin{cases} \frac{(\mu_j - \mu_i)}{b}, & \text{if } x < \mu_i \\ \frac{(2x - \mu_i - \mu_j)}{b}, & \text{if } \mu_i \leq x \leq \mu_j \\ \frac{(\mu_j - \mu_i)}{b}, & \text{if } x > \mu_j \end{cases} \quad (58)$$

This function is constant in the regions $x < \mu_i$ and $x > \mu_j$, and linear with slope $\frac{2}{b} > 0$ in the region $\mu_i \leq x \leq \mu_j$. Therefore, $h(x)$ is non-decreasing everywhere and strictly increasing in the middle region, making the density ratio $\exp(h(x)) = G_{c_i, c_j}(x)$ monotonic.

Similarly, when $\mu_i > \mu_j$, $h(x)$ has the form:

$$h(x) = \begin{cases} \frac{(\mu_j - \mu_i)}{b}, & \text{if } x < \mu_j \\ \frac{(-2x + \mu_i + \mu_j)}{b}, & \text{if } \mu_j \leq x \leq \mu_i \\ \frac{(\mu_j - \mu_i)}{b}, & \text{if } x > \mu_i \end{cases} \quad (59)$$

In this case, $h(x)$ is non-increasing everywhere and strictly decreasing in the middle region, making the density ratio $\exp(h(x)) = G_{c_i, c_j}(x)$ monotonic as well.

Thus, for Laplace distributions with identical scale parameters, the density ratio is always monotonic regardless of the ordering of the means. \square

D.2 Detection of Gaussian and Laplace cases

Algorithm 2 provides a procedure for determining whether two given samples S_1 and S_2 are drawn from either Gaussian or Laplace distributions with identical scale parameters. The algorithm employs both the Levene test for scale equality and Kolmogorov-Smirnov (KS) tests for distribution type identification.

The detection process consists of three main steps: First, a Levene test assesses whether both samples share the same scale parameter (lines 2-3). Second, KS tests determine whether each sample fits better to a Gaussian or Laplace distribution (lines 4-18). Finally, the algorithm combines both assessments to reach a conclusion about the samples (lines 19-34).

For each sample, the algorithm computes parameters for both Gaussian and Laplace fits, then applies KS tests to determine which distribution provides a better approximation. A sample is classified as Gaussian or Laplace based on whether the p -value exceeds the significance threshold α and whether it is higher than the p -value for the alternative distribution.

The algorithm returns a conclusion that considers both the scale equality and distribution type consistency. If both samples share the same scale and are consistently classified as either Gaussian or Laplace, the algorithm identifies them as having the same scale parameter with the specified distribution type.

The complete implementation is available in our code repository at <https://github.com/causal111/DRCD>.

Algorithm 2: Distribution Type and Scale Test (Levene Method)

Input: S_1, S_2 : Two samples to be tested, α : Significance level**Output:** Estimated distribution type and scale equivalence

```
1 function DistributionTest( $S_1, S_2, \alpha$ )
2   // Test for scale equivalence using Levene test
3    $L, p_L \leftarrow \text{Levene-Test}(S_1, S_2)$ 
4   // Test sample 1 for Gaussian and Laplace distribution
5    $\mu_1, \sigma_1 \leftarrow \text{Mean}(S_1), \text{StdDev}(S_1)$ 
6    $m_1, b_1 \leftarrow \text{Median}(S_1), \text{MeanAbsDev}(S_1)$ 
7    $p_{G1} \leftarrow \text{KS-Test}(S_1, \text{Gaussian}(\mu_1, \sigma_1))$ 
8    $p_{L1} \leftarrow \text{KS-Test}(S_1, \text{Laplace}(m_1, b_1))$ 
9   // Test sample 2 for Gaussian and Laplace distribution
10   $\mu_2, \sigma_2 \leftarrow \text{Mean}(S_2), \text{StdDev}(S_2)$ 
11   $m_2, b_2 \leftarrow \text{Median}(S_2), \text{MeanAbsDev}(S_2)$ 
12   $p_{G2} \leftarrow \text{KS-Test}(S_2, \text{Gaussian}(\mu_2, \sigma_2))$ 
13   $p_{L2} \leftarrow \text{KS-Test}(S_2, \text{Laplace}(m_2, b_2))$ 
14  // Determine distribution type based on p-values
15   $\text{isGauss}_1 \leftarrow (p_{G1} > \alpha) \wedge (p_{G1} > p_{L1})$ 
16   $\text{isLaplace}_1 \leftarrow (p_{L1} > \alpha) \wedge (p_{L1} > p_{G1})$ 
17   $\text{isGauss}_2 \leftarrow (p_{G2} > \alpha) \wedge (p_{G2} > p_{L2})$ 
18   $\text{isLaplace}_2 \leftarrow (p_{L2} > \alpha) \wedge (p_{L2} > p_{G2})$ 
19  if  $\text{isGauss}_1 \wedge \text{isGauss}_2$  then
20    distType  $\leftarrow$  Gaussian
21  else if  $\text{isLaplace}_1 \wedge \text{isLaplace}_2$  then
22    distType  $\leftarrow$  Laplace
23  else
24    distType  $\leftarrow$  Undetermined
25  // Final determination
26  if  $p_L > \alpha$  then
27    if distType = Gaussian then
28      return Same scale Gaussian distribution
29    else if distType = Laplace then
30      return Same scale Laplace distribution
31    else
32      return Same scale, but distribution type undetermined
33  else
34    return Different scales
```
